**Supplementary Figure 1. In vitro GCase activity and co-localization of GCase with LIMP-2 are not altered in Parkin KO cells.**

(**A**) In vitro GCase activity using 4-MUG substrate from WT and KO cell lysates. Two-tailed unpaired t-test, ns, not significant. n=3. a.u. arbitrary unit.

(**B**) Representative fluorescent images of GCase and LIMP-2 and quantification of mean fluorescence intensities of GCase and LIMP-2. Cells were fixed with cold methanol, and fixed cells were double immunostained with rabbit LIMP-2 and mouse GCase antibodies. Two-tailed unpaired t-test, n=13 microscopic fields from two coverslips for WT and 15 microscopic fields from two coverslips for KO cells. ns = p > 0.05, and quantitation of Pearson's correlation coefficient of GCase and LIMP-2. The Pearson's correlation coefficient were analyzed using Coloc2 plug-in (Fiji). Two-tailed unpaired t-test, n=10 images from two coverslips for WT and 10 images from two coverslips for KO. ns=p > 0.05.
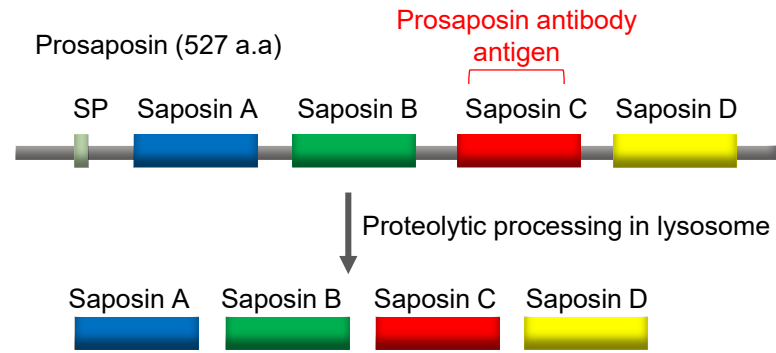
Supplementary Figure 2. Schematic representation of prosaposin cleavage into individual saposins (Saposin A, saposin B, Saposin C, and Saposin D). SP, signal peptide. Prosaposin antibody antigen is also shown.
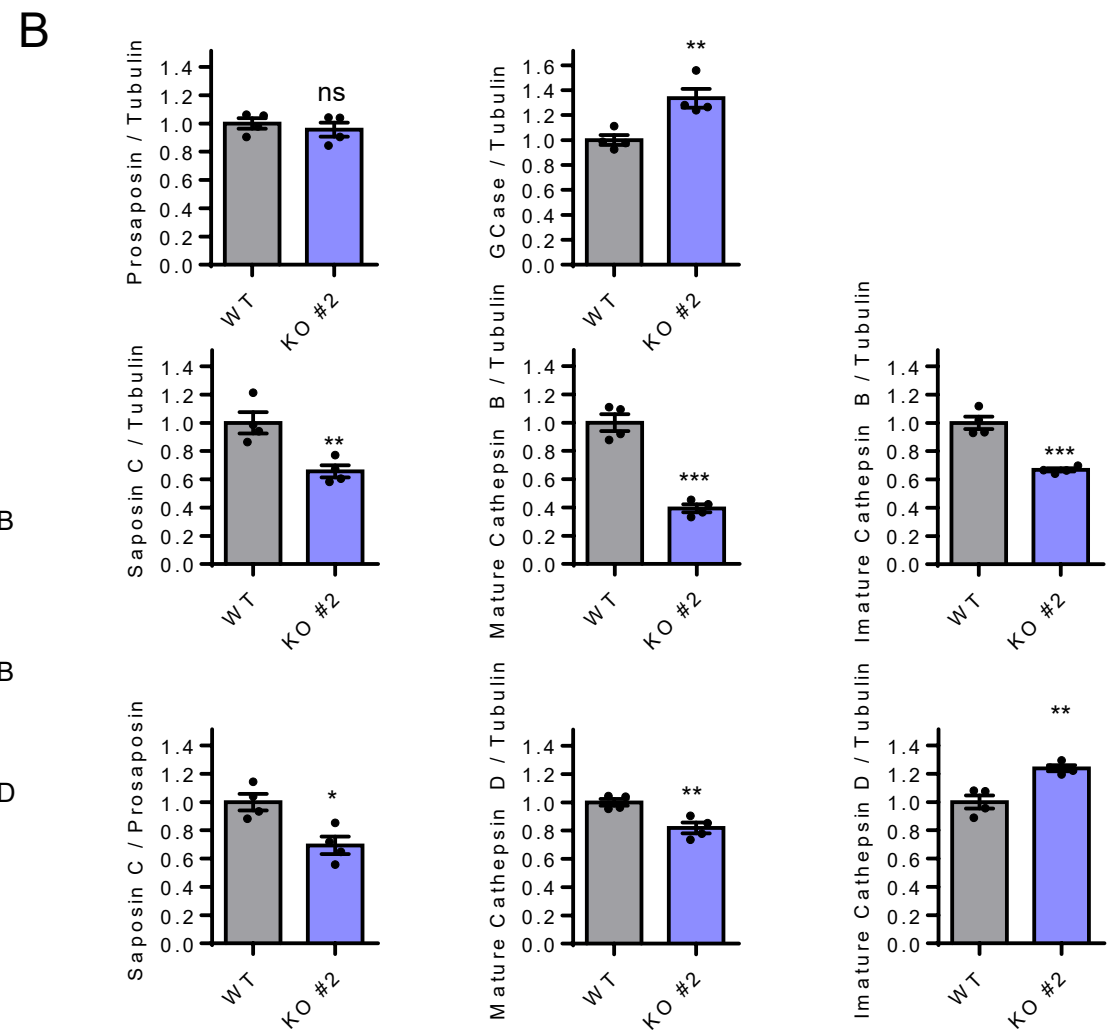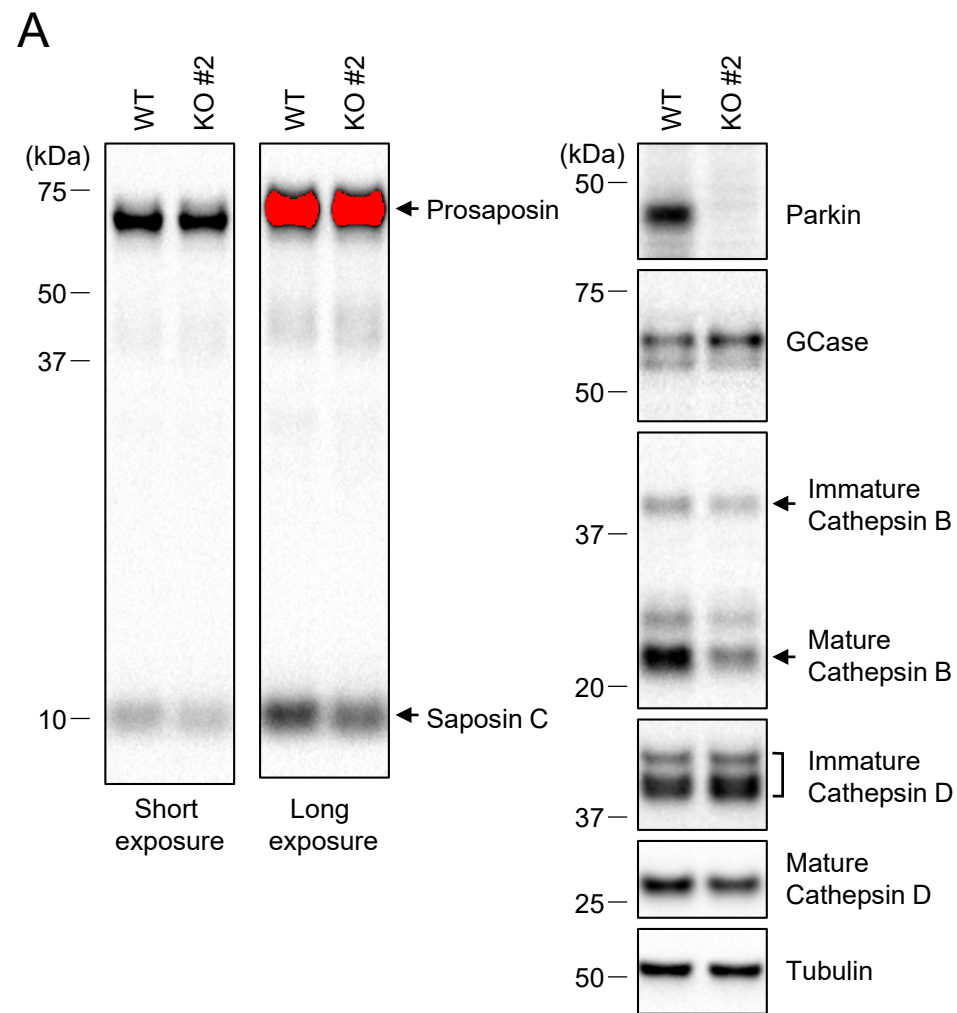
Supplementary Figure 3. Protein levels of saposin C and mature cathepsin B are reduced in independent Parkin knockout cell line (Parkin KO #2). Independent Parkin knockout cell line (Parkin KO #2) generated with different CRISPR guide RNA (target sequence, AGTGCCGTATTTGAAGCCTC) also shows reduced levels of cathepsin B and Saposin C. Protein levels of indicated proteins from total cell lysates from wild type HEK293-FT cell and Parkin KO #2 cells were analyzed with immunoblot. Representative immunoblot data are shown in (**A**). Saturated pixels are shown in red color. (**B**) Quantitation of immunoblot data. Band intensities are normalized with tubulin levels. Data are means ± SEM. Two-tailed unpaired t-test, n=4. * p< 0.05; ** p<0.01; *** p<0.001; ns, not significant.

Supplementary Figure 3

Supplementary Figure 4

Supplementary Figure 4. Effects of E64D on prosaposin, saposin C, cathepsin B and cathepsin D in WT and Parkin KO cell line.

(**A**) Quantitation of prosaposin, saposin c, Parkin, Cathepsin B, cathepsin D and tubulin upon PepstainA-ME (PepA-ME) treatment (4 μM, ~24hrs) in WT and KO cells. Protein band intensities were normalized to tubulin. n=3, two-way ANOVA with Tukey's multiple comparisons test, ns, not significant, ***$p < 0.001$.

(**A** and **B**) Representative immunoblots and quantitation of prosaposin, saposin c, Parkin, cathepsin B, cathepsin D and tubulin upon treatment with membrane-permeant cysteine protease inhibitor (E64D, 20 μM, ~24hrs) in WT and KO cells. Band intensities were normalized to tubulin. n ≥ 3, two-way ANOVA with Tukey's multiple comparisons test, *$p < 0.05$, **$p < 0.01$, ***$p < 0.001$, ns, not significant.
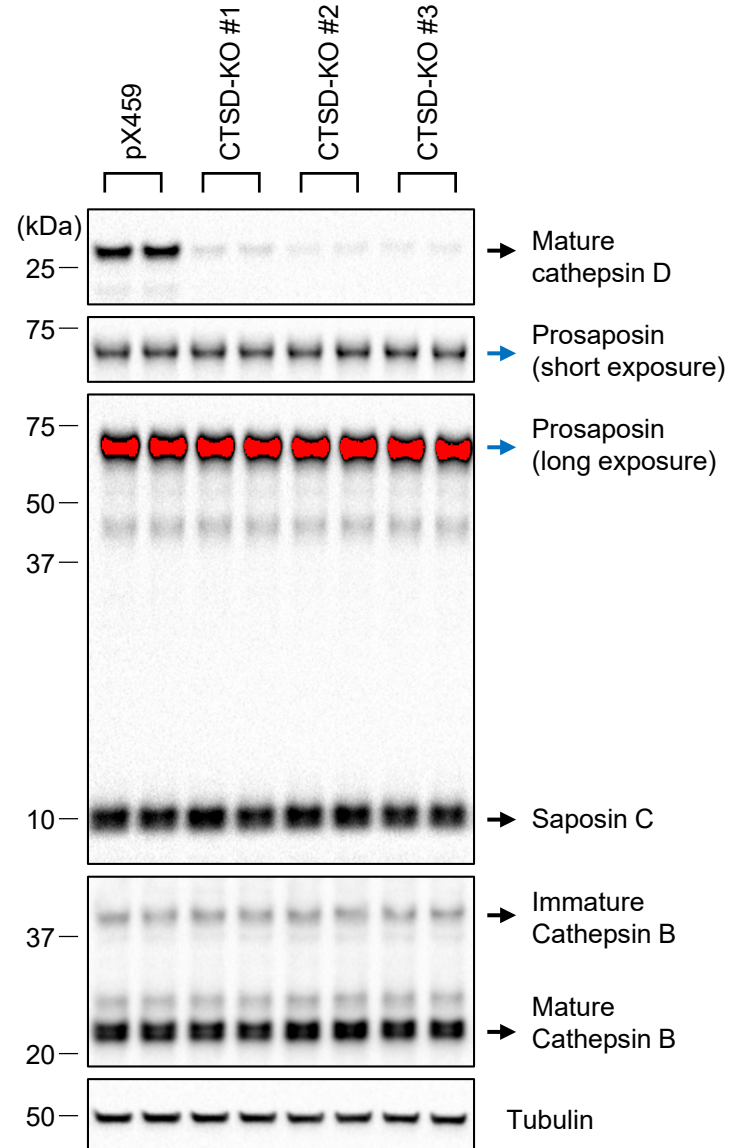
Supplementary Figure 5
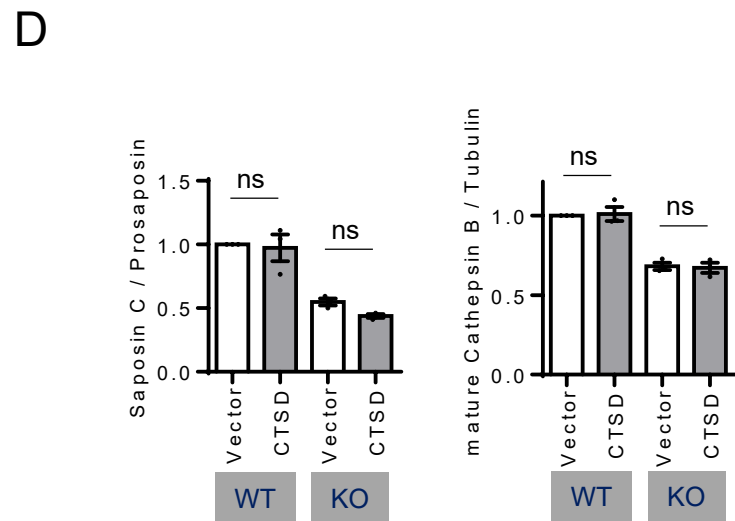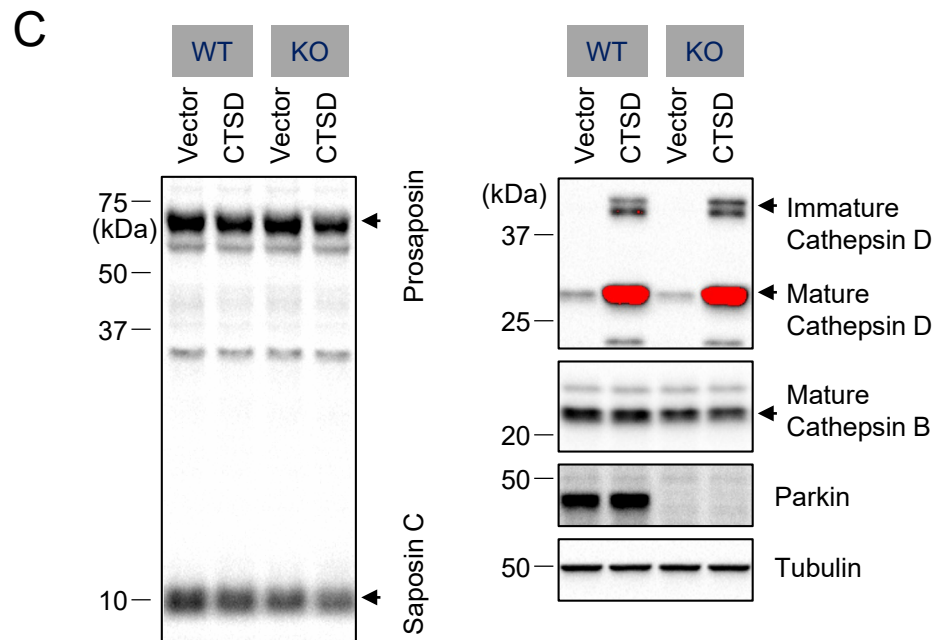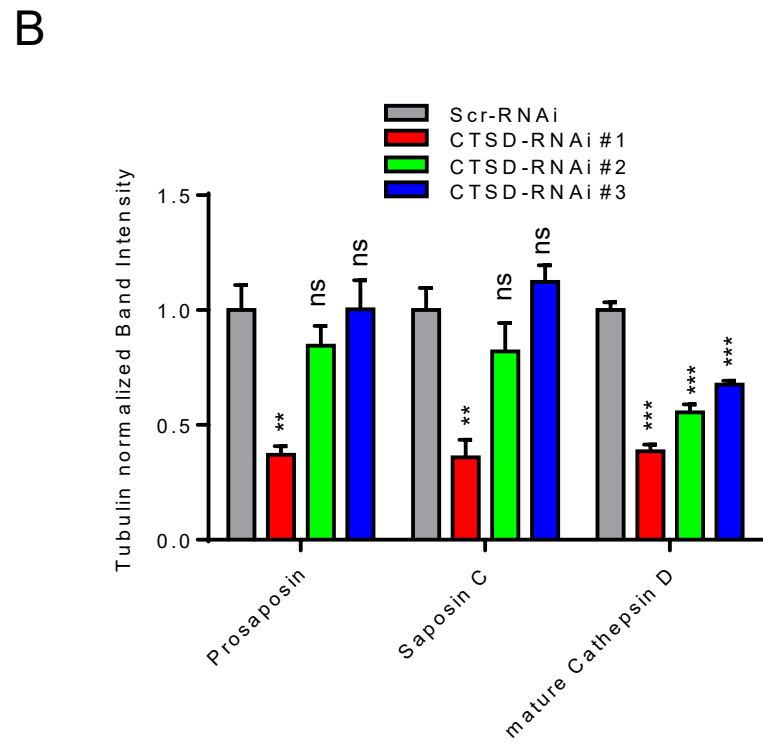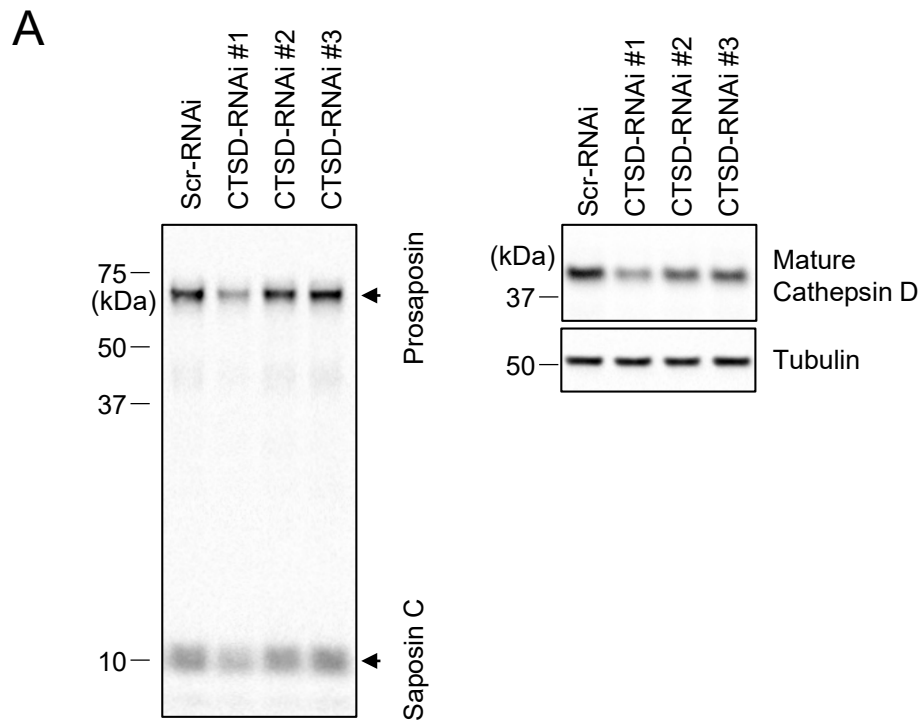
Supplementary Figure 5. Cathepsin D does not play a major role in prosaposin processing.

(**A**) Representative immunoblot data of indicated proteins upon RNAi knockdown of cathepsin D in HEK293-FT cells. As a control, scrambled RNAi (Scr-RNAi) was used, and three independent cathepsin D RNAi constructs (CTSD-RNAi #1 and CTSD-RNAi #2, CTSD-RNAi #3) were tested.

(**B**) Quantitation of indicated proteins upon cathepsin D knockdown. Band intensities were normalized to tubulin, and compared to scrambled RNAi (Scr-RNAi) transfected HEK293-FT cells. n=3, *p < 0.05, **p < 0.01, ***p < 0.001, ns, not significant. One-way ANOVA with Tukey's multiple comparisons test.

(**C** and **D**) Representative immunoblot data of indicated proteins upon cathepsin D (CTSD) overexpression in WT or KO cells, and quantitation of saposin to prosaposin ratio and mature cathepsin B upon Cathepsin D overexpression. Band intensities were normalized to tubulin, and compared to vector transfected WT cells. Two-tailed unpaired t-test within same cell line, n=3, ns, not significant.
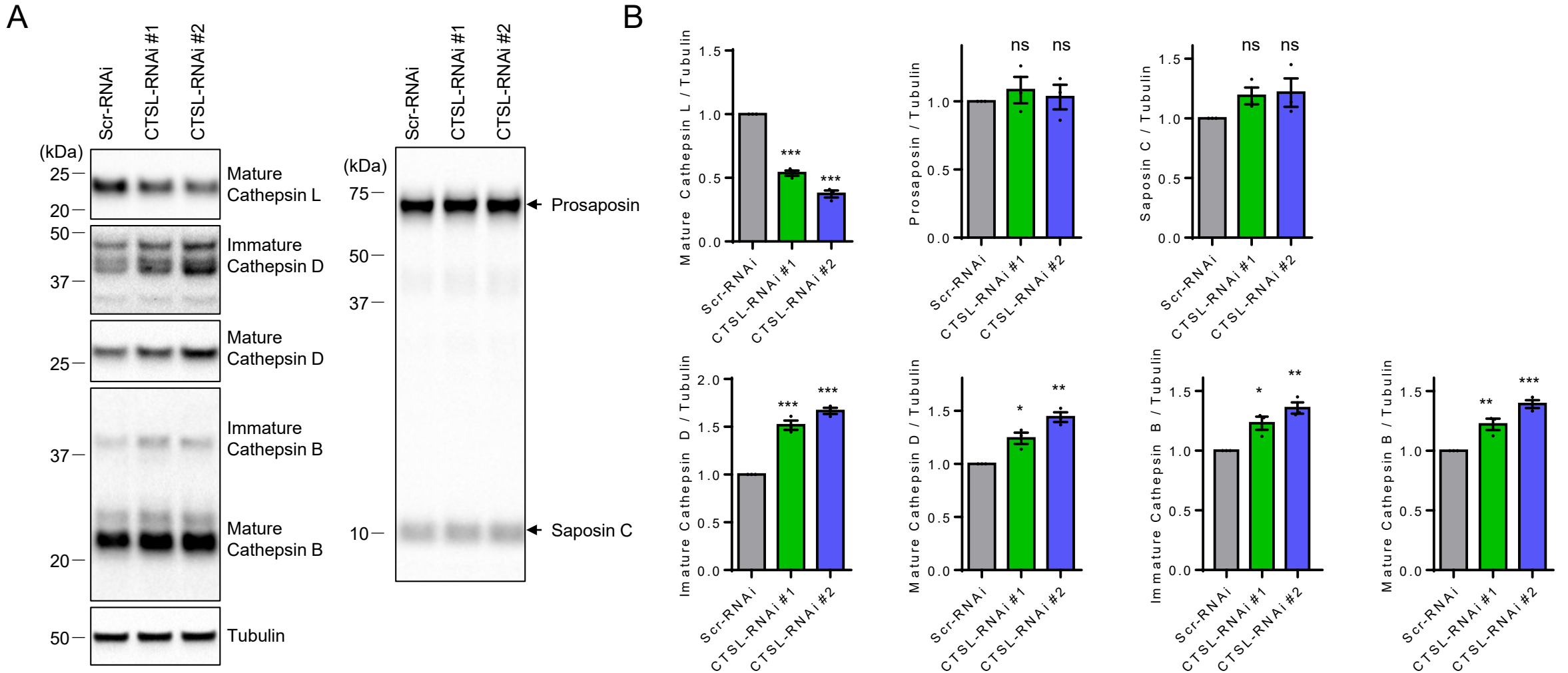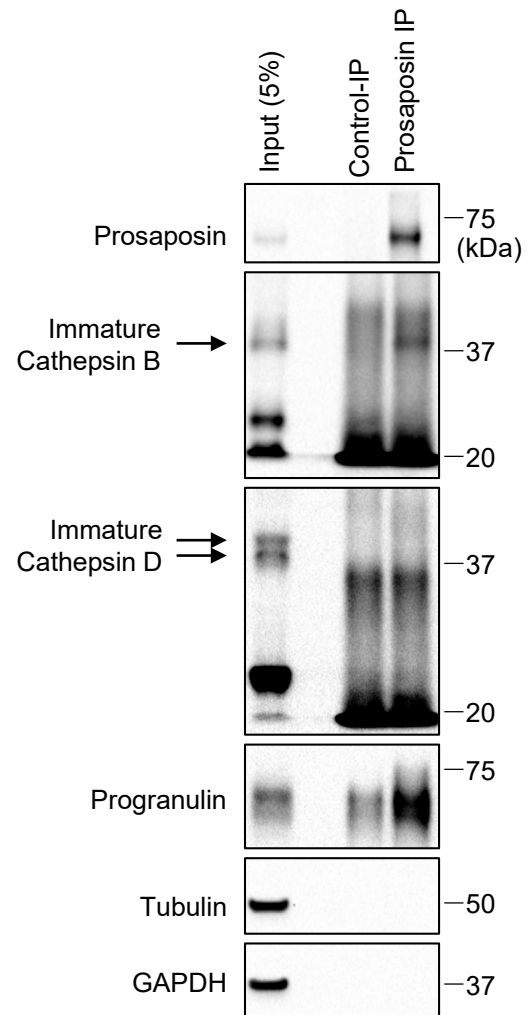
Supplementary Figure 6
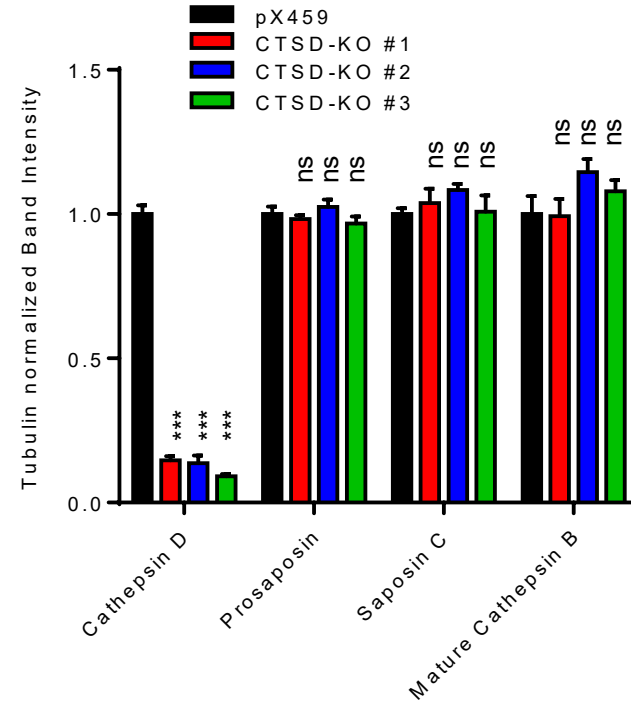
Supplementary Figure 6. Three independent heterogeneous CTSD-knockout cell pools do not show any significant changes in prosaposin processing or cathepsin B maturation.

(**A**) Representative immunoblot data of indicated proteins in control cells transfected with empty CRISPR/Cas9 vector (pX459) and three independent heterogeneous CTSD-knockout cell pools (CTSD-KO#1 and CTSD-KO#2, CTSD-KO#3). HEK293-FT cell line were transfected with either empty CRISPR/Cas9 vector (pX459) or pX459 vectors harboring gRNA targeting CTSD (pX459-CTSD KO#1 (target sequence, TCTCCTTCTACCTGAGCAGG), pX459-CTSD KO#2 (target sequence, CGTTGTTGACGGAGATGCGG) , or pX459-CTSD KO#3 (target sequence, TGGGCGGTGTCAAAGTGGAG). One day after transfections, transfected cells were selected with puromycin (2.5μg/ml) for two days. Puromycin-resistant cells were harvested and re-plated onto 12-well plate with cell density of ~100,000 cells per well, and cultured for additional three days without puromycin. Cells were then harvested and analyzed with immunoblot using indicated antibodies. (**B**) Quantitation of indicated proteins in heterogeneous CTSD-knockout cell pools. Band intensities were normalized to tubulin, and compared to HEK293-FT cells transfected with pX459. One-way ANOVA followed by Dunnett's test. n=4, ***$p < 0.001$, ns, not significant.

Supplementary Figure 7. RNAi knockdown of endogenous cathepsin L does not affect prosaposin processing.

HEK293-FT cells were transfected with either scrambled RNAi (Addgene plasmid #10878) or human cathepsin L-RNAi constructs (CTSL-RNAi#1 (TRCN0000318682) and CTSL-RNAi #2 (TRCN0000318611)). Two days later, transfected cells were harvested and analyzed with immunoblot using indicated antibodies. Representative immunoblot data are shown in (**A**). (**B**) Quantitation of immunoblot data. Band intensities are normalized with tubulin levels. Data are means ± SEM. Repeated-measures ANOVA with Tukey's post hoc analysis. n=3. * p< 0.05; ** p<0.01; *** p<0.001; ns, not significant.
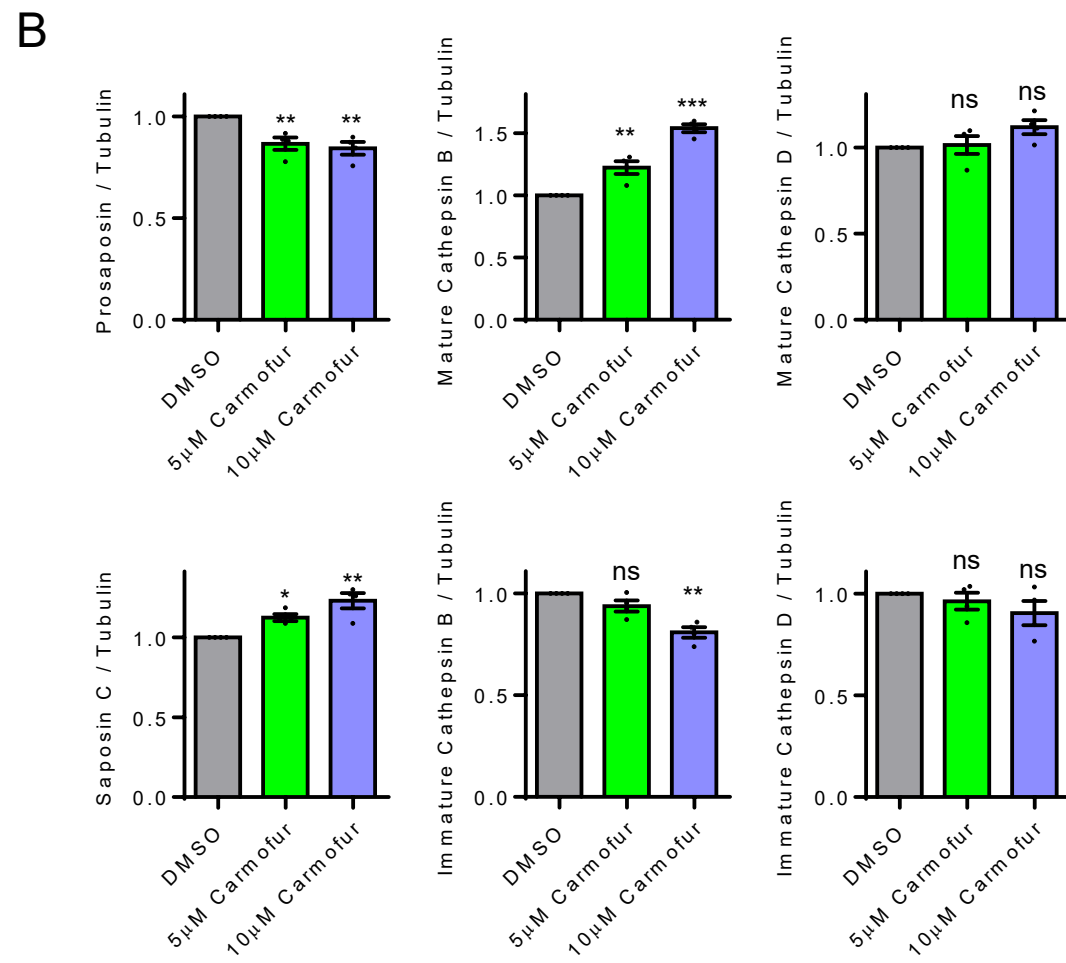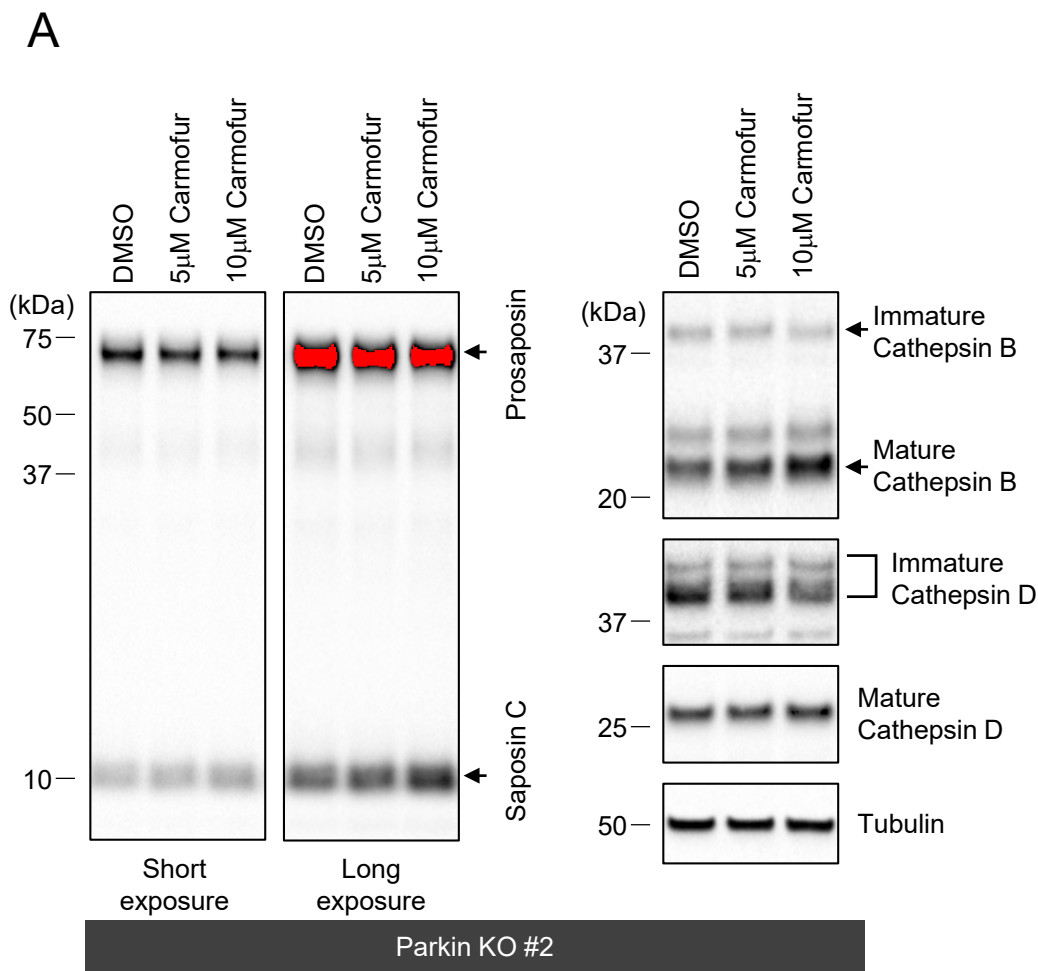
Supplementary Figure 8. Prosaposin co-immunoprecipitates with immature form of cathepsin B.

Representative immunoblot data from co-immunoprecipitation assay. HEK293-FT cells lysates were immunoprecipitated with either control HA-antibody or prosaposin antibody. Isolated prosaposin immune-complexes were analyzed with immunoblot using indicated antibodies. Three independent co-immunoprecipitation experiments produced similar data.
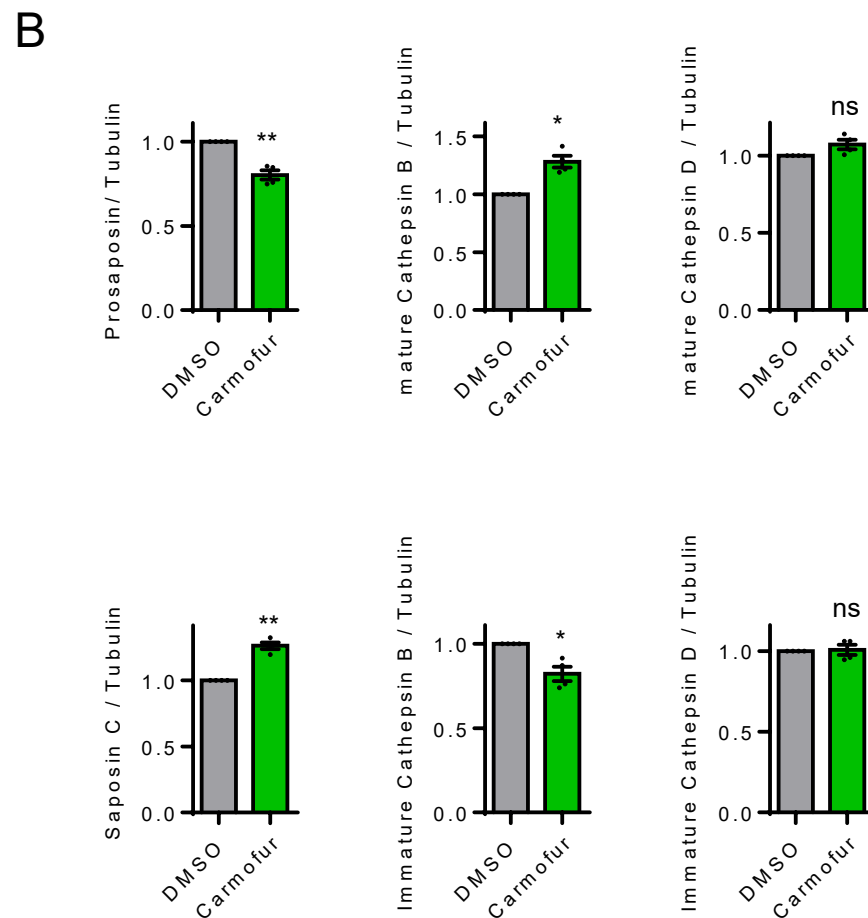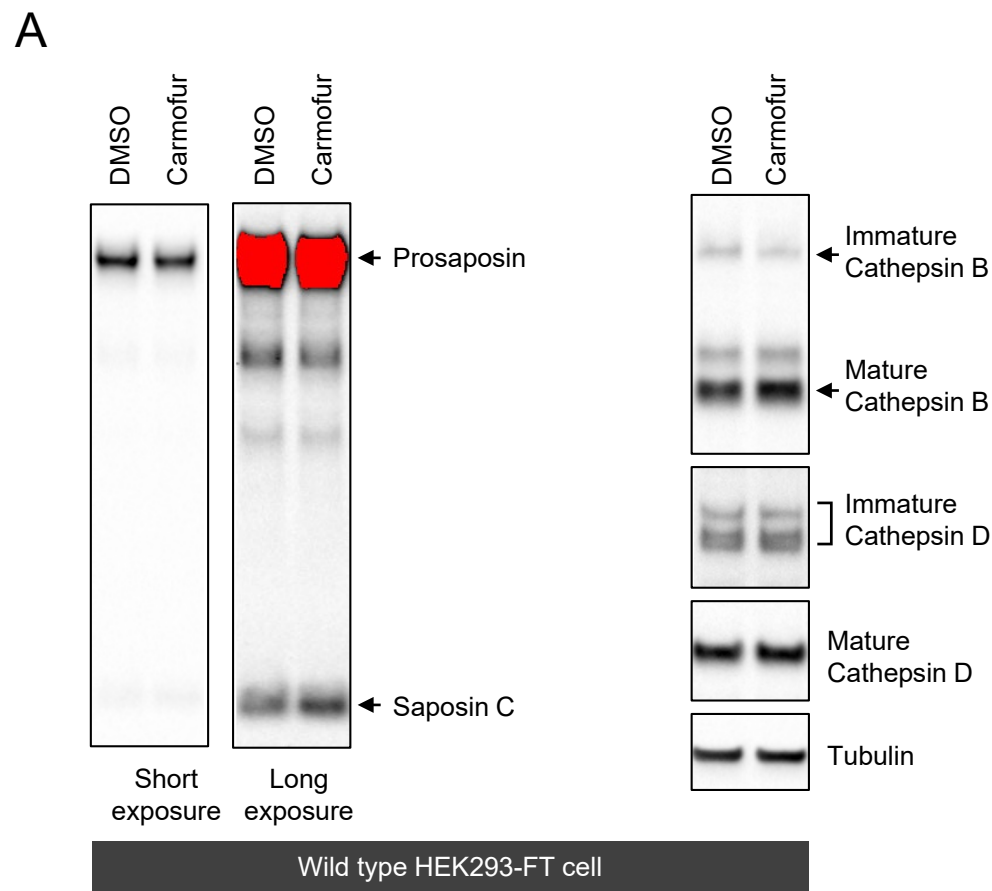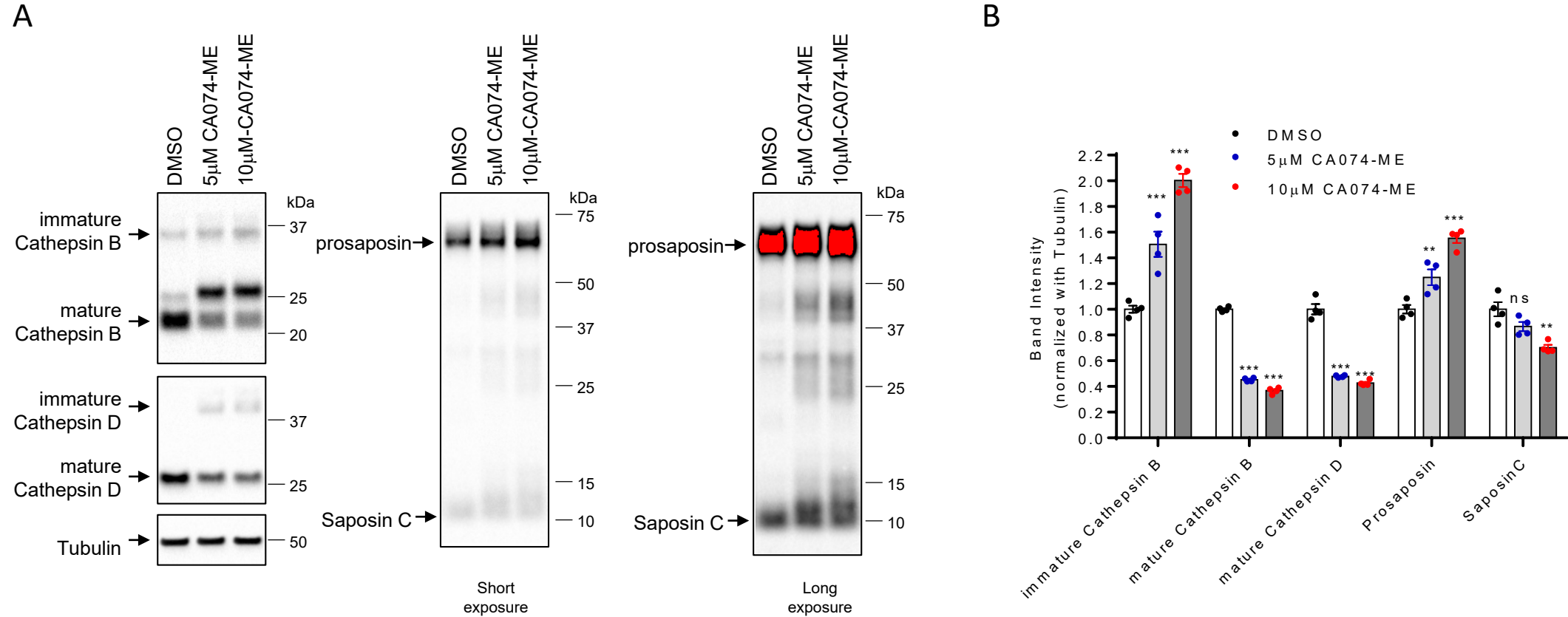
Supplementary Figure 9. Carmofur treatment in WT HEK293-FT cells promotes cathepsin B maturation and prosaposin processing to saposin C.

WT HEK293-FT cells were treated either with DMSO or 5μM carmofur for ~16hrs. Lysates from treated cells were analyzed with immunoblot. Representative immunoblot data are shown in (**A**). (**B**) Quantitation of immunoblot data. Band intensities are normalized with tubulin levels. Data are means ± SEM. Paired t-test. n=4. * p< 0.05; ** p<0.01; ns, not significant.
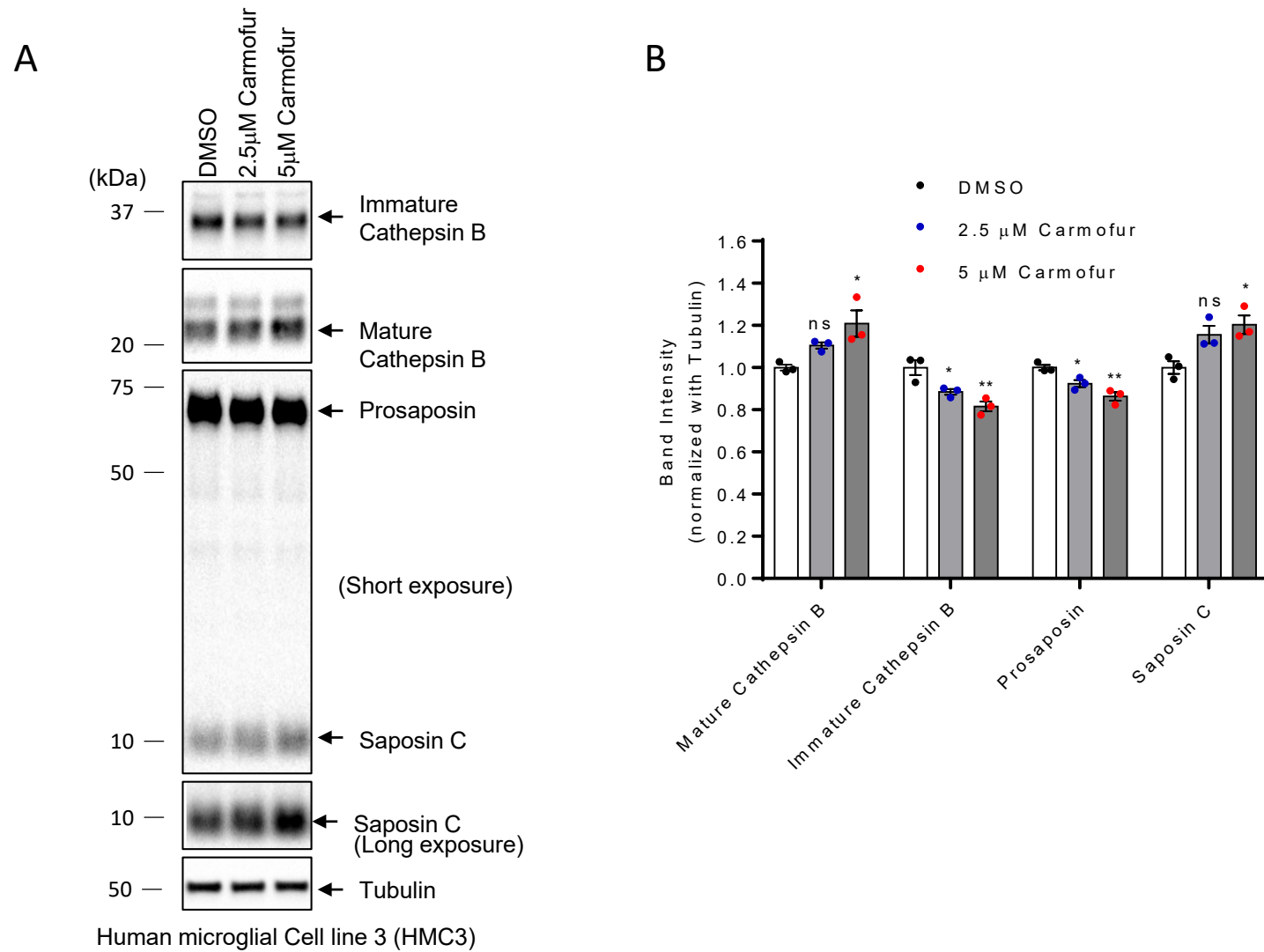
Supplementary Figure 10. Carmofur treatment in the Parkin KO #2 cell line generated with different CRISPR/Cas9 guide RNA also promotes cathepsin B maturation and prosaposin processing to saposin C.

Parkin KO #2 cells were treated either with DMSO or carmofur (5μM or 10μM) for ~16hrs. Lysates from treated cells were analyzed with immunoblot. Representative immunoblot data are shown in (**A**). (**B**) Quantitation of immunoblot data. Band intensities are normalized with tubulin levels. Data are means ± SEM. Repeated-measures ANOVA with Tukey's post hoc analysis. n=4. * p< 0.05; ** p<0.01; *** p<0.001; ns, not significant.

Supplementary Figure 11. CA074-ME, cathepsin B inhibitor, treatment in Human Microglial cell line 3 (HMC3) impairs cathepsin B maturation and prosaposin processing to saposin C. Human microglial cell line 3 (HMC3) cells (ATCC, CRL-3304) were treated with DMSO, 5μM, or 10μM CA074-ME for ~40hrs. Lysates from treated cells were analyzed with immunoblot. Representative immunoblot data are shown in (**A**). (**B**) Quantitation of immunoblot data. Band intensities are normalized with tubulin levels. Data are means ± SEM. One-way ANOVA with Dunnett's Post Hoc test. n=4. ** p< 0.01; *** p<0.001; ns, not significant.

Supplementary Figure 12. Carmofur treatment in Human Microglial Cell line 3 (HMC3) promotes cathepsin B maturation and prosaposin processing to saposin C. Human microglial cell line 3 (HMC3) cells (ATCC, CRL-3304) were treated with DMSO, 2.5µM, or 5µM carmofur for ~16hrs. Lysates from treated cells were analyzed with immunoblot. Representative immunoblot data are shown in (**A**). (**B**) Quantitation of immunoblot data. Band intensities are normalized with tubulin levels. Data are means ± SEM. One-way ANOVA with Dunnett's Post Hoc test. n=3. * p< 0.05; ** p<0.01; ns, not significant.
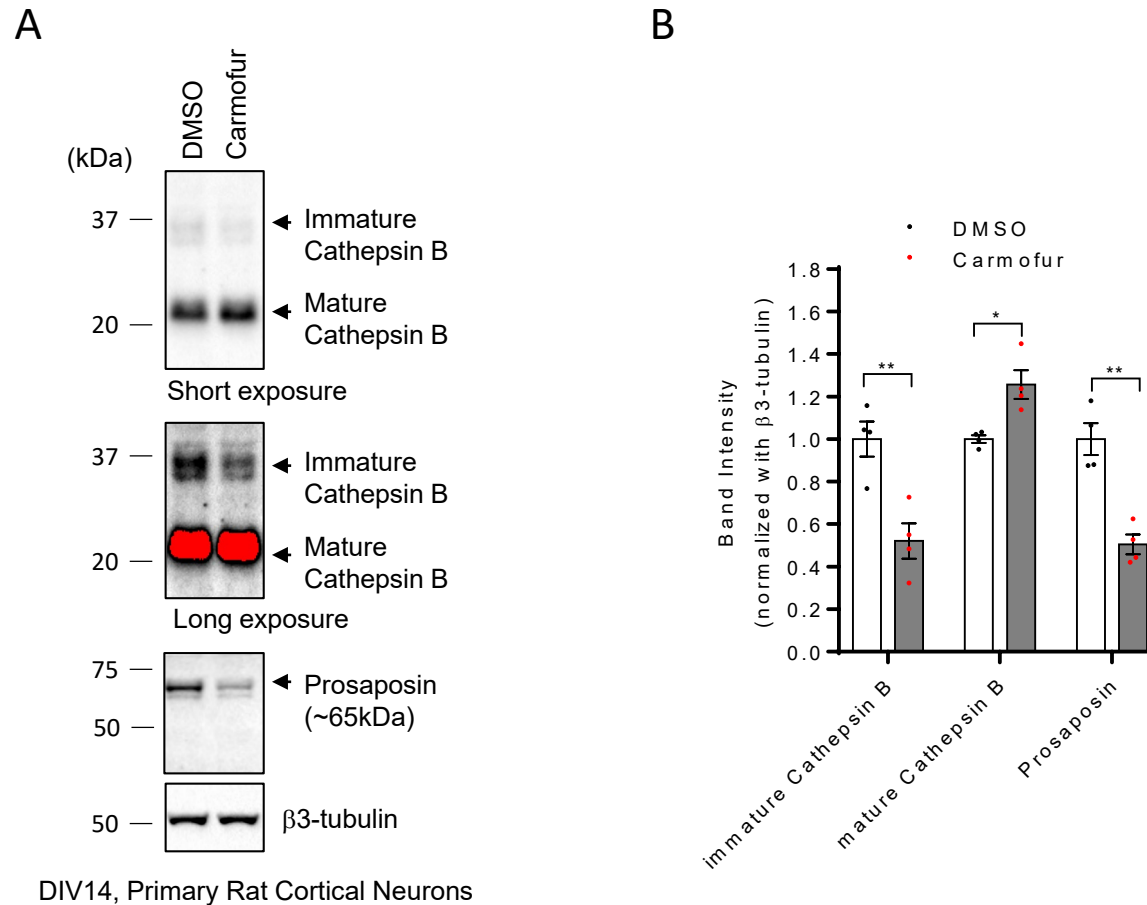
Supplementary Figure 13. Chemical inhibition of acid ceramidase inhibitor with carmofur in rat primary cortical neurons increases mature forms of cathepsin B, and promote prosaposin cleavage. (A) Representative immunoblot data showing effects of carmofur treatment (7.5μM for ~20hrs) in rat primary cortical neurons (DIV13) on cathepsin B and prosaposin. DMSO treatment was used as a control. Primary cortical neuronal cultures prepared from embryonic day 19 rat embryos. Cells were plated on 12-well plate coated with poly-D-lysine (10 μg/ml) at a density of 150,000/well. Protein samples were analyzed with immunoblot using cathepsin B (AF953, R&D systems), prosaposin (AF8520, R&D systems) and β3-tubulin antibody (Cat# 802001, BioLegend). (B) Quantitation of effects of carmofur treatment in rat primary cortical neurons. Protein band intensities were normalized with β3-tubulin. Two-tailed unpaired t-test, n=4, **<0.01, *<0.05.

Supplementary Figure 14
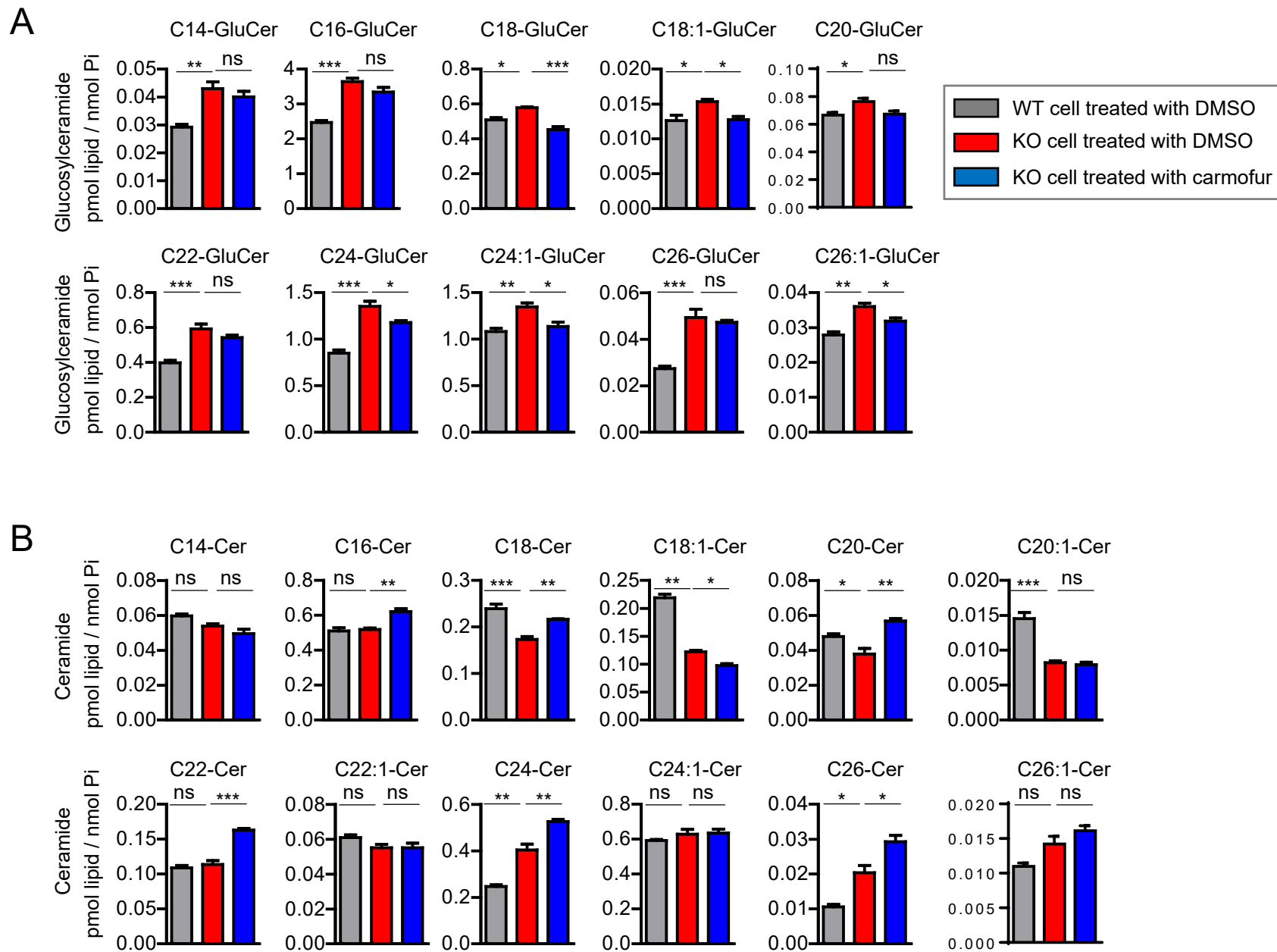
Supplementary Figure 14. Lipidomic analysis of glucosylceramide and ceramide in WT cell and KO cells and effects of carmofur on glucosylceramide and ceramide in KO cells.

(**A**) Lipidomic analysis of Glucosylceramide species (GluCer) in WT cell and KO cells and effects of carmofur on glucosylceramide species in KO cells. Glucosylceramide were quantified and expressed as p mol / n mole inorganic phosphate (Pi). $*p < 0.05$, $**p < 0.01$, $***p < 0.001$, ns, not significant, One-way ANOVA followed by Tukey's multiple comparisons test. n=3.

(**B**) Lipidomic analysis of ceramide species (Cer) in WT cell and KO cells and effects of carmofur on ceramide species in KO cells. Ceramide species were quantified and expressed as p mol / n mole inorganic phosphate (Pi). $*p < 0.05$, $**p < 0.01$, $***p < 0.001$, ns, not significant, One-way ANOVA followed by Tukey's multiple comparisons test. n=3.
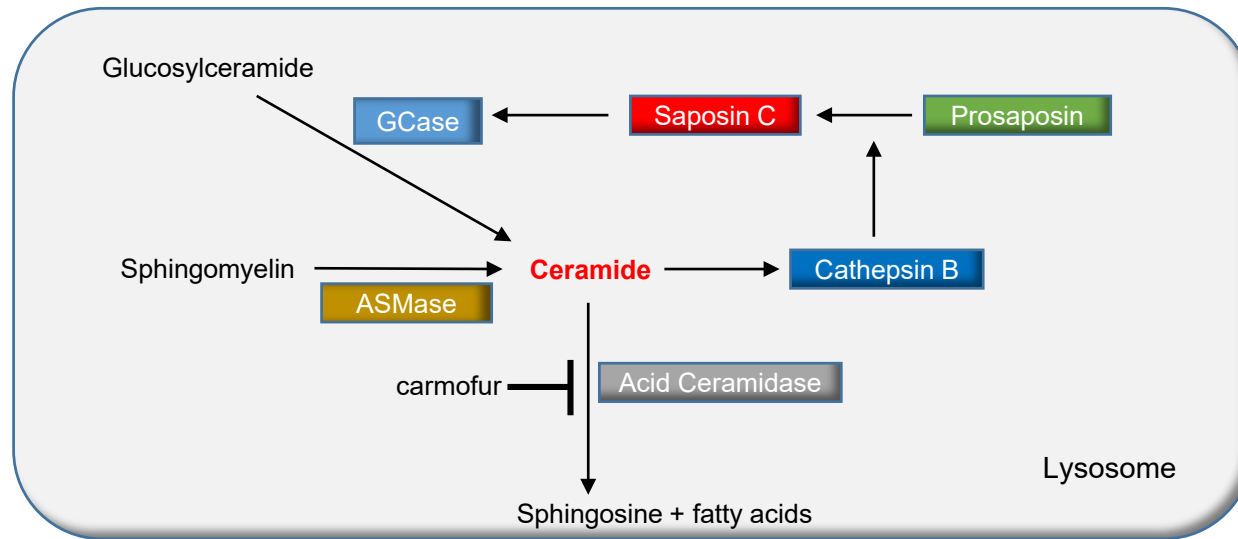
Supplementary Figure 15. A model of lysosomal ceramide promoted cathepsin B activation and prosaposin processing to saposin C.
Lysosomal ceramides are generated by the lysosomal β-glucocerebosidase (GCase) or acid sphingomyelinase (ASMase). Lysosomal ceramides activates cathepsin B to promote prosaposin processing to saposin C, a GCase activator in lysosomes. Acid ceramidase converts lysosomal ceramides into sphingosines and fatty acid. Carmofur, acid ceramidase inhibitor, increases lysosomal ceramide levels to promote cathepsin B activation and subsequent prosaposin processing to saposin C.